

Cooling and heating regions of Joule-Thomson expansion for AdS black holes: Maxwell-power-Yang-Mills and Kerr Sen black holes

Jafar Sadeghi ^{*1}, Mohammad Reza Alipour ^{*2} Saeed Noori Gashti^{†,*3},
Mohammad Ali S. Afshar ^{*4}

^{*}Department of Physics, Faculty of Basic Sciences,
University of Mazandaran P. O. Box 47416-95447, Babolsar, Iran

[†]School of Physics, Damghan University, P. O. Box 3671641167, Damghan, Iran

Abstract

In this paper, we explore the Joule-Thomson expansion (JTE) process for the Einstein-Power-Young-Mills (EPYM) and the AdS Kerr Sen (AKS) black holes. We study the effect of free parameters on the Joule-Thomson coefficient (JTC), the inversion curve, and the T_i^{min}/T_c . The isenthalpic curves of the AKS black hole show cooling or heating behavior depending on the inversion curve, which is affected by the mass and the parameters b and a of the black hole. If we assume the parameter b to be zero, the results reduce to the Kerr-AdS black holes [1]. In [2,3], for the Einstein-Power-Yang-Mills AdS black hole with $q > 1$ and $n = 2$, the T_i^{min}/T_c is $1/2$. But in this paper, for the AdS-Maxwell-power-Yang-Mills black hole, when $q > 1$, the T_i^{min}/T_c is almost equal to $1/2$ for the increase of Maxwell's charge C , and when $q = 1/2$, the T_i^{min}/T_c is equal to $1/2$ for all values of C . Also, when $1/2 < q < 1$, the T_i^{min}/T_c is close to the value of $1/2$, and finally when $0 < q < 1/2$, the values of T_i^{min}/T_c move away from the value of $1/2$, that is, they become smaller. For the AKS black hole, we found that for free parameters $a = 0.00951$ and $b = 0.00475$, the T_i^{min}/T_c is almost $1/2$. Finally, we compare our findings with others in the literature and summarize our results in Tables 1-5.

Keywords: JTE, AdS-Maxwell-power-Yang-Mills black holes, AdS Kerr Sen black holes

Contents

1	Introduction	2
2	Joule-Thomson expansion	3
3	Case I: AdS-Maxwell-power-Yang-Mills black holes	5

¹Email: pouriya@ipm.ir

²Email: mr.alipour@stu.umz.ac.ir

³Email: saeed.noorigashti@stu.umz.ac.ir

⁴Email: m.a.s.afshar@gmail.com

4	Case II: AdS-Kerr-Sen black hole	6
5	Discussion and results	9
5.1	Case I	9
5.2	Case II	14
6	Conclusion	19

1 Introduction

The insights provided by astronomy, astrophysics, and experimental cosmology suggest that cosmic structures adhere to the same principles and foundations observed on Earth, albeit with minor variations and necessary simplifications. This structural and fractal similarity is a crucial tool for human ideation and cognition, enabling us to decode more aspects of this global pattern daily. Researchers leverage this understanding in hypothesizing theoretical models, which may not yet be empirically verifiable. They construct various models based on mathematical logic and physical laws, exploring all potential scenarios to predict the most plausible ideas consistent with the formation of the enigmatic, infinite universe. The existing black hole models, are actually one of the most obvious examples of this form of inference. Despite being one of the most elusive cosmic entities, they are studied based on this pattern. The comparison of a black hole’s gravitational behavior with a thermodynamic ensemble in the 1970s gave rise to a significant branch of black hole physics, namely black hole thermodynamics. For instance, the four laws of black hole mechanics bear a striking resemblance to the laws of thermodynamics [4,5]. Similarly, a black hole’s surface area is analogous to entropy in thermodynamics, and its surface gravity is comparable to temperature [4,5]. The introduction of Maldacena duality, also known as the AdS/CFT correspondence, established a deeper connection between black hole thermodynamics and this duality, offering profound insights into quantum gravity. In the context of AdS/CFT, a black hole’s entropy in the bulk AdS space correlates with the entropy of the corresponding CFT on the boundary, known as the Bekenstein-Hawking entropy [6]. Moreover, the black hole’s temperature is related to the CFT’s temperature [6–9].

This correspondence provides a powerful tool to study the quantum aspects of gravity and black holes using the methods of quantum field theory. In AdS space, there is a Hawking-Page phase transition between a stable large black hole and a thermal gas [10]. This phase transition is a first-order transition that occurs when the temperature of the system reaches a critical value, where the free energy of the black hole becomes lower than that of the thermal gas [10]. This phase transition can be interpreted as a confinement deconfinement phase transition of a gauge field [11]. The Hawking-Page phase transition can be seen as a transition from a deconfined phase in the thermal gas to a confined phase in the black hole [11]. When the AdS black holes have electric charge, they exhibit rich phase structures that were studied by Chamblin et al [12,13]. They found that the phase transition behavior of charged AdS black holes resembles the liquid-gas phase transition in a van der Waals system [14]. In the extended phase space where the cosmological constant is treated as pressure [15], the P-V critical behavior of charged AdS black holes was investigated and it was shown that they have a similar analogy to the van der Waals liquid-gas system. In addition to the phase transition and critical phenom-

ena [16–23], the analogy between the black holes and the van der Waals system was also creatively applied to the well-known JTE process [24] recently. This means that the JTC can be used to study the thermodynamics of black holes as well. For example, the isenthalpic expansion process is the analogue of the JTE process for black holes, where the black hole mass is constant while the black hole pressure and volume are changed. The black hole pressure is related to the cosmological constant, and the black hole volume is related to the horizon radius. In this case, the inversion curve is the curve that separates the regions where the black hole temperature increases or decreases as the pressure decreases. One of the intriguing features of the inversion curves for black hole systems is that they have only positive slopes, unlike the van der Waals system, which has both positive and negative slopes. For example, for charged AdS black holes [24] and Kerr-AdS black holes [1], the isenthalpic expansion process and the inversion curve have been analyzed and observed that the inversion curve was found to have a positive slope, meaning that the black hole temperature always decreases as the pressure decreases. Then the analysis was generalized to other types of AdS black holes, such as quintessence charged AdS black holes [25], holographic superfluids [26], charged AdS black holes in $f(R)$ gravity [27], AdS black holes with a global monopole [28], and AdS black holes in Lovelock gravity [29]. For further study, you can see also [2, 30–38].

All the results showed that the inversion curves for all these black hole systems have only positive slopes. We are interested in exploring whether this feature is universal for all black hole systems, or whether there are other effects that can alter it. To this end, we will focus on two types of AdS black holes: AdS-Maxwell-power-Yang-Mills and AdS Kerr Sen. These black holes have additional parameters that can affect their thermodynamic behavior and phase transitions. AdS-Maxwell-power-Yang-Mills black holes are black holes that have a non-linear electromagnetic field, which is described by a power-law function of the field strength [39]. This field can be seen as a generalization of the Maxwell field, which is the standard model of electromagnetism. AdS Kerr Sen black holes are black holes that have electric charge and angular momentum in a low-energy limit of heterotic string theory [40]. This theory is a type of string theory that combines the features of bosonic and supersymmetric strings. These black holes have different properties and characteristics than the standard AdS black holes, such as the existence of a dilaton field, which is a scalar field that couples to the electromagnetic field and the curvature. We will investigate how these parameters affect the inversion curves and the JTE process for these black holes, and compare them with the previous results for other black hole systems.

The structure of this paper is as follows. In Sec.II, we give a brief overview of the JTE. In Sec.III and Sec.IV, We introduce briefly AdS-Maxwell-Power-Yang-Mills and the AdS Kerr Sen black holes and their thermodynamic properties. In Sec.V, we study the JTE process for these black holes, derive an explicit expression for the JTC, and analyze and discuss the effect of the parameters of each model on the inversion curves. In Sec.VI, we present our conclusion and discussion.

2 Joule-Thomson expansion

In classical thermodynamics, a throttling process or the JTE process, discovered in 1852, is a method of cooling or heating a system by changing its pressure and volume, without adding or removing heat. In this process, the

high-pressure gas passes through a porous plug into a region with a low pressure, while keeping the enthalpy constant. Since it is a constant-enthalpy process, it can be used to experimentally measure the lines of constant enthalpy (isenthalps) on the (p, T) diagram of a system. Combined with the specific heat capacity at constant pressure, it allows the complete measurement of the thermodynamic potential for the gas [41].

In this method, The main goal is to investigate the behavior of the coefficient that describes the temperature change during the expansion or compression of a system at constant enthalpy, which is denoted by μ and is known as the JTC,

$$\mu = \left(\frac{\partial T}{\partial P}\right)_H = \frac{1}{C_P} \left[T \left(\frac{\partial V}{\partial T}\right)_P - V \right].$$

If the above coefficient is positive, as a result of pressure reduction, the temperature will decrease. In other words, the expansion of the gas causes cooling and the compression of the gas under investigation causes it to heat up. In other words, the positive JTC indicates the same direction of temperature and pressure. Whereas, if the JTC is negative, a decrease in pressure causes an increase in temperature.

The JT inversion temperature, which is determined by setting $\mu = 0$, is the temperature at which the sign of the JTC changes. Most real gases have an inversion point. The temperature of this point depends on the gas pressure before expansion.

$$T_i = V \left(\frac{\partial T}{\partial V}\right)_P.$$

The important point is that if you plot the JTC on the (p,T) diagram, a closed parabolic curve is created. In simpler terms, the inversion temperature is placed on the boundary of the curve of temperature changes in terms of pressure. At this temperature, the JTC changes from negative to positive. At a given pressure, the isopressure-temperature line intersects the drawn curve at two different points. These two points are called low temperature and high temperature of inversion. In fact, at temperatures higher and lower than these two temperatures, the sign of the JTC is negative and between these two temperatures, the sign of the JTC is positive. According to the above, the interesting phenomenon in this process is that the (p, T) diagram has two regions: one where the gas cools down and one where the gas heats up. These regions are separated by the inversion curve, the curve that shows the points where the system temperature does not change during the expansion process, that divides the graph into two regions: the cooling region and the heating region. The cooling region is where the gas temperature decreases as the pressure decreases, and the heating region is where the gas temperature increases as the pressure decreases. The inversion curve depends on the type of the gas and its initial conditions. If with respect to zero coefficient for ideal gases, we choose the van der Waals system, which is a more realistic model than the ideal gas, and takes into account the finite size and the attractive forces of the molecules, we find that for the van der Waals system, the inversion curves have both positive and negative slopes, forming a circle in the pressure axis. The inversion curve for the van der Waals system has a negative slope in the low-pressure region, where the attractive forces dominate, and a positive slope in the high-pressure region, where the repulsive forces dominate.

3 Case I: AdS-Maxwell-power-Yang-Mills black holes

The AMPYM black holes are rooted in the study of black hole solutions in the context of supergravity theories, especially in anti-de Sitter (AdS) space. The study of black holes in AdS space is important for various reasons, including its relevance to string theory and the AdS/CFT correspondence, which is a duality between gravitational theories in AdS space and field theories defined on its boundary. These black holes are solutions to the equations of motion of supergravity theories with additional matter fields, such as Maxwell fields and power-Yang-Mills fields, within the context of AdS space that arises from a generalization of the Einstein-Maxwell theory with a negative cosmological constant and a non-Abelian gauge field. The history of AMPYM black holes can be traced back to the discovery of the first black holes in Einstein-Yang-Mills theory, which were considered in the works of Yasskin [42] and Kasuya [43]. It should be noted that in the non-Abelian case there are various gauge groups, but to obtain black hole solutions it is necessary to choose a specific form for the gauge potential. One of the simplest forms that nevertheless allowed to derive interesting and important results is the so-called Wu-Yang ansatz, which leads to magnetic-type solutions. [44–47]. Of course, an interesting point that can be mentioned is that the primary black holes with non-Abelian fields, which were studied in the late 80s [48–51], were found to be unstable in the case of asymptotically flat geometry [52, 53], but later black hole solutions were obtained in the AdS case, which were shown to be stable [54–57]. The AMPYM black holes have been extensively studied in the context of theoretical physics, particularly in the context of holography and its applications to understanding strongly coupled field theories. In recent years, the study of AMPYM black holes has continued to be an active area of research, with a focus on understanding their thermodynamic properties, phase transitions, and connections to gauge/gravity duality. These black holes have been studied as models for strongly coupled systems in the dual field theories, providing valuable insights into nonperturbative phenomena in quantum field theories. Researchers have investigated various aspects of AMPYM black holes, such as their stability, entropy, and critical behavior. Their thermodynamic properties have been of particular interest, as they exhibit rich phase structures and can undergo phase transitions similar to those observed in condensed matter systems. Furthermore, the holographic interpretation of these black holes has led to fruitful connections between gravitational physics and field theory, shedding light on fundamental questions in quantum gravity and strongly coupled systems [58–60]. This section provides a summary of the thermodynamics of N-dimensional Einstein-Maxwell-power-Yang-Mills gravity with a cosmological constant Λ . This theory of gravity is based on the following action, which we will explain in more details. So we will have,

$$I = \frac{1}{2} \int dx^N \sqrt{-g} \left(R - \frac{(N-1)(N-2)\Lambda}{3} - F_{\mu\nu} F^{\mu\nu} - (Tr(F_{\mu\nu}^{(a)} F^{(a)\mu\nu}))^q \right). \quad (1)$$

The trace element is represented by $Tr(\cdot) = \sum_{a=1}^{(N-1)(N-2)/2} (\cdot)$, with R as the Ricci scalar and q as a real positive parameter. The Yang-Mills and Maxwell fields are defined accordingly [4],

$$F_{\mu\nu}^{(a)} = \partial_\mu A_\nu^{(a)} - \partial_\nu A_\mu^{(a)} + \frac{1}{2\sigma} C_{(b)(c)}^{(a)} A_\mu^b A_\nu^c, \quad (2)$$

$$F_{\mu\nu} = \partial_\mu A_\nu - \partial_\nu A_\mu, \quad (3)$$

$C_{(b)(c)}^{(a)}$ represents the structure constants of the $(N-1)(N-1)/2$ parameter Lie group G , while σ denotes the coupling constant. $A_\mu^{(a)}$ refers to the $SO(N-1)$ gauge group Yang-Mills potentials, with A_μ representing the conventional Maxwell potential [39]. The metric solution corresponding to the N -dimensional spherically symmetric line element is as follows [40],

$$ds^2 = -f(r)dt^2 + \frac{1}{f(r)}dr^2 + r^2 d\Omega_n^2. \quad (4)$$

The $d\Omega_n^2$ denotes the volume of the unit n -sphere. In this study, we will direct our attention to the Einstein-Maxwell-power-Yang-Mills theory (*EMPYM*) with $N(=n+2) \geq 4$ and $q \neq (n+1)/4$. The solution to the N -dimensional *EMPYM* black hole with a negative cosmological constant under the condition of $q \neq \frac{n+1}{4}$ is provided [39],

$$f(r) = 1 - \frac{2m}{r^{n-1}} - \frac{\Lambda r^2}{3} + \frac{2(n-1)C^2}{nr^{2(n-1)}} + \frac{Q}{r^{4q-2}} \quad (5)$$

$$Q = \frac{[n(n-1)Q_1^2]^q}{n(4q-n-1)}.$$

It is important to note that the parameter m represents the mass of the black hole, while C and Q_1 denote the charges of the Maxwell field and Yang-Mills field, respectively. In the extended phase space, the cosmological constant is considered as a thermodynamic pressure $P = -\frac{\Lambda}{8\pi}$, in this case, the Hawking temperature, mass and entropy of the black hole are obtained as follows,

$$T = -\frac{C^2(n-1)^2}{2\pi nr_+^{2n-1}} + \frac{2}{3}(n+1)Pr_+ - \frac{Q(-n+4q-1)}{4\pi r_+^{4q-1}} + \frac{n-1}{4\pi r_+}, \quad (6)$$

$$M = \frac{n\omega_n}{48\pi} \left(\frac{6C^2(n-1)}{nr_+^{n-1}} + 8\pi Pr_+^{n+1} + 3Qr_+^{n-4q+1} + 3r_+^{n-1} \right), \quad (7)$$

$$S = \frac{\omega_n r_+^n}{4}, \quad \omega_n = \frac{2\pi^{\frac{n+1}{2}}}{\Gamma\left(\frac{n+1}{2}\right)}, \quad (8)$$

where r_+ and ω_n are the horizon radius and the volume of the unit n -sphere respectively.

4 Case II: AdS-Kerr-Sen black hole

The Kerr-Sen-AdS black hole is a complex and fascinating topic in the field of theoretical physics. It is a type of rotating, charged black hole that emerges from heterotic string theory. It is a generalization of the Kerr-Newman-AdS black hole, which is a solution of the Einstein-Maxwell equations with a negative cosmological constant. The Kerr-Sen-AdS black hole also involves a dilaton and an axion field, which are scalar and pseudoscalar fields that appear in string theory [61]. The first exact solution of the Einstein field equations, known as the

Schwarzschild solution, was discovered by Karl Schwarzschild in 1916. This solution describes a simple, non-rotating, uncharged black hole. The next major advancement came in 1963, when Roy P. Kerr found a solution to the Einstein field equations that describes a rotating black hole. This was a significant development, as it is believed that most black holes in the universe are rotating. In 1965, Ezra Newman and his collaborators found a solution that describes a rotating, charged black hole, known as the Kerr-Newman black hole. This solution was later extended by Ashoke Sen to include a dilaton field and an axion field, resulting in the Kerr-Sen black hole. The AdS form of this black hole was first derived by Ashoke Sen in 1992, by applying a series of duality transformations to the Kerr-Newman-AdS black hole. Sen showed that the Kerr-Sen-AdS black hole retains some of the symmetries and properties of the Kerr-Newman-AdS black hole, such as the existence of an event horizon, an ergosphere, and a Penrose process. However, the Kerr-Sen-AdS black hole also has some unique features, such as the dependence of the mass and angular momentum on the dilaton charge, and the violation of the cosmic censorship conjecture for some values of the parameters [61]. The Kerr-Sen-AdS black hole solution is a specific example of a rotating black hole with additional fields, which is of particular interest due to the role of angular momentum and the presence of nontrivial matter content in the spacetime geometry and is a solution to the equations of motion of supergravity theories with additional matter fields, such as the Sen-type dilaton and antisymmetric tensor fields, within the context of AdS space.

The properties and thermodynamics of Kerr Sen-AdS black holes have been the subject of intense research, given their relevance to understanding the behavior of rotating black holes in the presence of nontrivial matter content and their implications for the AdS/CFT correspondence [62–72]. The study of Kerr Sen-AdS black holes has been motivated by theoretical developments in string theory, quantum gravity, and holography, as well as by their potential implications for gravity dualities and the behavior of strongly coupled systems in the dual field theories. This black hole has been studied from various perspectives, including its thermodynamic properties, stability, and connections to the dynamics of dual field theories. In recent years, there has been growing interest in exploring the dynamical behavior of Kerr Sen-AdS black holes, including their evolution, instability, and the connections to chaos and information loss puzzles. Researchers have investigated the behavior of these black holes under various perturbations and have sought to understand their implications for fundamental questions about black hole thermodynamics and the fate of information in quantum gravity. Moreover, the holographic interpretation of Kerr Sen-AdS black holes has led to fruitful connections between gravitational physics and field theory, shedding light on fundamental questions in quantum gravity and strongly coupled systems [62–72]. In summary, the history and ongoing research on Kerr Sen-AdS black holes represent a rich and interdisciplinary area of study that has fruitful connections to diverse fields of theoretical physics, including string theory, quantum gravity, holography, and nonlinear dynamics. The exploration of these black holes continues to be an exciting frontier for probing the fundamental nature of spacetime and its connections to quantum theory. In this section provides a short overview of the Kerr-Sen black hole and its generalization to the anti-de Sitter spacetimes. Sen [61] found a solution of the low-energy effective action of the heterotic string theory, which describes a charged rotating black hole, known as the Kerr-Sen black hole. The action is a modification of the general relativity action with additional fields from the heterotic string theory, given by [62, 78],

$$S = \int d^4x \sqrt{-\tilde{g}} e^{-\Phi} \left[\mathcal{R} + (\nabla\Phi)^2 - \frac{1}{8}F^2 - \frac{1}{12}H^2 \right], \quad (9)$$

where \tilde{g} is the determinant of the metric tensor $g_{\mu\nu}$, \mathcal{R} is the Ricci scalar, $F = F_{\mu\nu}F^{\mu\nu}$ with $F_{\mu\nu}$ being the $U(1)$ Maxwell field strength tensor, Φ is a scalar dilaton field, and $H = H_{\mu\nu\rho}H^{\mu\nu\rho}$ is the field strength for the axion field. The action can be transformed to the Einstein frame by a conformal transformation of the metric:

$$ds_E^2 = e^{-\Phi} d\tilde{s}^2. \quad (10)$$

The action in the Einstein frame is given by:

$$S = \int d^4x \sqrt{-g} \left[R - \frac{1}{2}(\nabla\Phi)^2 - \frac{e^{-\Phi}}{8}F^2 - \frac{e^{-2\Phi}}{12}H^2 \right]. \quad (11)$$

The metric of a Kerr-Sen-AdS black hole in Boyer-Lindquist coordinates is given by [62, 78]:

$$ds^2 = -\frac{\Delta_r}{\rho^2} \left(dt - \frac{a \sin^2 \theta}{\Xi} d\phi \right)^2 + \frac{\rho^2}{\Delta_r} dr^2 + \frac{\rho^2}{\Delta_\theta} d\theta^2 + \frac{\sin^2 \theta \Delta_\theta}{\rho^2} \left[-\frac{(r^2 + 2br + a^2)}{\Xi} d\phi + adt \right]^2, \quad (12)$$

where

$$\begin{aligned} \rho^2 &= r^2 + a^2 \cos^2 \theta + 2br, \\ \Delta &= (r^2 + 2br + a^2) \left(1 + \frac{r^2 + 2br}{\ell^2} \right) - 2mr, \\ \Xi &= 1 - \frac{a^2}{\ell^2}, \\ \Delta_\theta &= 1 - \frac{a^2}{\ell^2} \cos^2 \theta. \end{aligned} \quad (13)$$

The parameter b is the dyonic charge of the black holes and is expressed as $b = q^2/(2m)$, where q is the electric charge and m is the mass of the black holes. In the limit of $\ell \rightarrow \infty$, the metric reduces to the usual Kerr-Sen black holes. The non-rotating case ($a = 0$) reduces to the Gibbons-Maeda-Garfinkle-Horowitz-Strominger (GMGHS) solution. Gibbons and Maeda [73, 74] found the black hole and black brane solutions in the dilaton theory, and Garfinkle-Horowitz-Strominger obtained their charged version [75]. It is worth mentioning that the Kerr-Sen-AdS black holes in four dimensions have been explored from various aspects, such as the black hole shadows [76] and the phase space thermodynamics in the extended phase space [77]. The ADM mass M , the angular momentum J , and the charge Q in AdS spacetimes are related by,

$$\begin{aligned} M &= \frac{m}{\Xi^2}, \\ J &= \frac{ma}{\Xi^2}, \\ Q &= \frac{q}{\Xi}. \end{aligned} \quad (14)$$

Also, the entropy is given by,

$$S = \frac{A}{4} = \frac{\pi(r_+^2 + 2br + a^2)}{\Xi}, \quad (15)$$

where r_+ is the radius of the event horizon, which is the largest root of $\Delta = 0$. When $b=0$, the thermodynamic quantities become the same as those of Kerr-AdS black holes. Kerr-AdS black holes are solutions of the Einstein field equations in four dimensions with negative cosmological constant and rotation.

5 Discussion and results

In this section, we investigate the JTE process for AdS black holes: AMPYM and AdS Kerr Sen and derive a clear formula for the JTC. We also examine how the charge and the parameters of AMPYM and Kerr-Sen theories affect the inversion curves. We also compare the inversion curves for different scenarios

5.1 Case I

In this section, we explore the JTE of black hole systems in the extended phase space, where the black hole mass M is the same as the enthalpy H . We compare this process with the JT process of van der Waals gases with fixed particle number, and we use the fixed charge Q for the black hole systems. We also assume that the other parameters are constant. Using [2, 45] as a reference, and considering the mass of black holes, we can write the pressure P as a function of M and r_+ , the mass and the horizon radius of a black hole. By substituting this expression in the temperature formula, we can obtain the temperature as a function of M and r_+ as well. Furthermore, we can express the mass M and the temperature T in terms of the pressure P and the radius r_+ of a black hole. Therefore, we get,

$$P(M, r_+) = -\frac{3\left(\frac{2C^2(n-1)r_+^{-2n}}{n} + Qr_+^{-4q} + \frac{1}{r_+^2}\right)}{8\pi} + \frac{6Mr_+^{-n-1}}{n\omega_n}. \quad (16)$$

Also, we have T in terms of M and r_+ as follows,

$$T(M, r_+) = -\frac{2C^2(n-1)r_+^{2-2n} + 2qQr_+^{2-4q} + 1}{2\pi r_+} + \frac{4M(n+1)r_+^{-n}}{n\omega_n}. \quad (17)$$

By solving the above equations, one can obtain the function $T(M, P)$, which is lengthy and will not be shown here. For particular free parameters for this model, the $T(M, P)$ curve can be shown. According to the definition of the JTC $\mu = \left(\frac{\partial T}{\partial P}\right)_M$, the inversion pressure and temperature between the cooling and heating regions are (\tilde{P}, \tilde{T}) , which are determined by $\mu = 0$. Therefore, the most important thing is to find the function expression of μ . By setting $\mu = 0$, one can obtain the inversion points (\tilde{P}, \tilde{T}) for different fixed enthalpy M . With respect to [24], the JTC is given by,

$$\mu = \left(\frac{\partial T}{\partial P}\right)_M = \frac{1}{C_P} \left[T \left(\frac{\partial V}{\partial T}\right)_P - V \right]. \quad (18)$$

This approach is elegant. However, in this paper, we will use more straightforward methods by applying only mass and temperature to derive the JTC μ . we can see that temperature is a function of pressure and radius,

and radius is a function of pressure and mass. So, the JTC is given by,

$$\mu = \left(\frac{\partial T}{\partial P}\right)_M = \frac{\partial_{,r_+} T}{\partial_{,r_+} P}. \quad (19)$$

Now, using the relationship $\mu = \frac{\partial T}{\partial P}|_M = \frac{\frac{\partial T}{\partial r_+}}{\frac{\partial P}{\partial r_+}}$, we calculate Joule Thomson coefficient as follows,

$$\mu = \frac{2nr_+ (\omega_n (r_+^{4q} (2C^2 (2n^2 - 3n + 1) r_+^2 + r_+^{2n}) + 8q^2 Q r^{2n+2} - 2qQ r_+^{2n+2}) - 8\pi M(n+1)r_+^{n+4q+1})}{3 (n\omega_n (r_+^{4q} (2C^2(n-1)r_+^2 + r_+^{2n}) + 2qQ r_+^{2n+2}) - 8\pi M(n+1)r_+^{n+4q+1})}. \quad (20)$$

When the value of the coefficient μ is positive during the expansion, it means that the temperature decreases and therefore it is called a cooling phenomenon. However, when μ is negative, the temperature increases, and this is called a heating process. Using various equations, we can write the mass M and the temperature T as functions of the pressure P and the radius r_+ , which are the properties of a black hole. For $\mu = 0$, we can obtain the inversion temperature, in which the process of the temperature changes reverses. It can be obtained by the formula,

$$T_i = V \left(\frac{\partial T}{\partial V}\right)_P, \quad (21)$$

$$V = \frac{\partial M}{\partial p} = \frac{1}{6} n r_+^{n+1} \omega_n. \quad (22)$$

At the inversion temperature, the value of μ is 0, and the inversion temperature is determined by the following equation:

$$T_i = V \frac{\partial T}{\partial V} = V \frac{\frac{\partial T}{\partial r_+}}{\frac{\partial V}{\partial r_+}}. \quad (23)$$

This is beneficial for identifying the areas of heating and cooling in the $T - P$ plane. We calculate t using the equations (17), (20), (21), (22) and (23),

$$T_i = \frac{r_+ \left(\frac{6C^2(n-1)^2(2n-1)r_+^{-2n}}{n} + 8\pi(n+1)P_i + 3(1-4q)Q(n-4q+1)r_+^{-4q} + \frac{3-3n}{r_+^2} \right)}{12\pi(n+1)}. \quad (24)$$

We can also have from relation (17),

$$T_i = \frac{-\frac{6C^2(n-1)^2 r_+^{1-2n}}{n} + 8\pi(n+1)r_+ P_i + 3Q(n-4q+1)r_+^{1-4q} + \frac{3(n-1)}{r_+}}{12\pi}. \quad (25)$$

Figure 1 displays the Hawking temperature as a function of the horizon. We keep the free parameters constant for each plot. In each subfigure, we can observe some zero points for different free parameters. These zero points correspond to the divergence points of the JTC, as we can easily see in figure 1. According to the radius

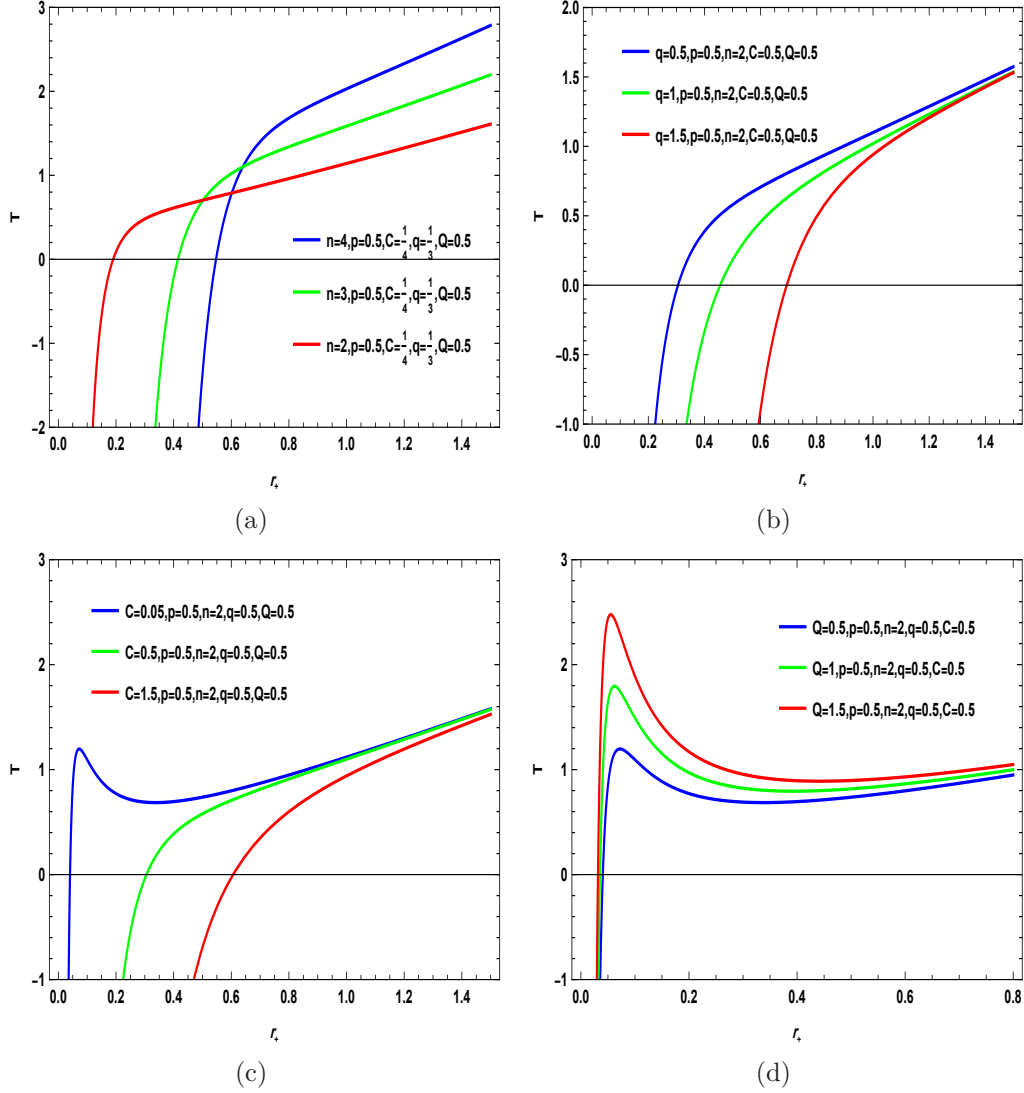


Figure 1: It shows the plot of $(T - r_+)$ for the AMPYM black hole with respect to free parameters that are determined in each plot

of the horizon and the values of free parameters of a black hole, for small values for the radius of the event horizon, our structural behavior is completely distinct, and for larger radii, the figures almost converge. We have plotted the isenthalpic curves and the inversion curve of the AMPYM black hole for various values of the free parameter in each plot of Figure 2. In every subfigure, two isenthalpic curves with different values of M , along with the corresponding inversion curve that occurs at the highest point of the isenthalpic curves. We denote the inversion temperature and pressure of each isenthalpic curve as T_i and P_i , respectively. The isenthalpic curves are divided into two regions by the inversion curve: for $P < P_i$, the isenthalpic curve has

a positive slope, indicating that the black hole undergoes cooling during the expansion process. However, for $P > P_i$, the isenthalpic curve has a negative slope, implying that the black hole experiences heating during the expansion process. This behavior is consistent for different values of the free parameter in Figures (2a-2b). We

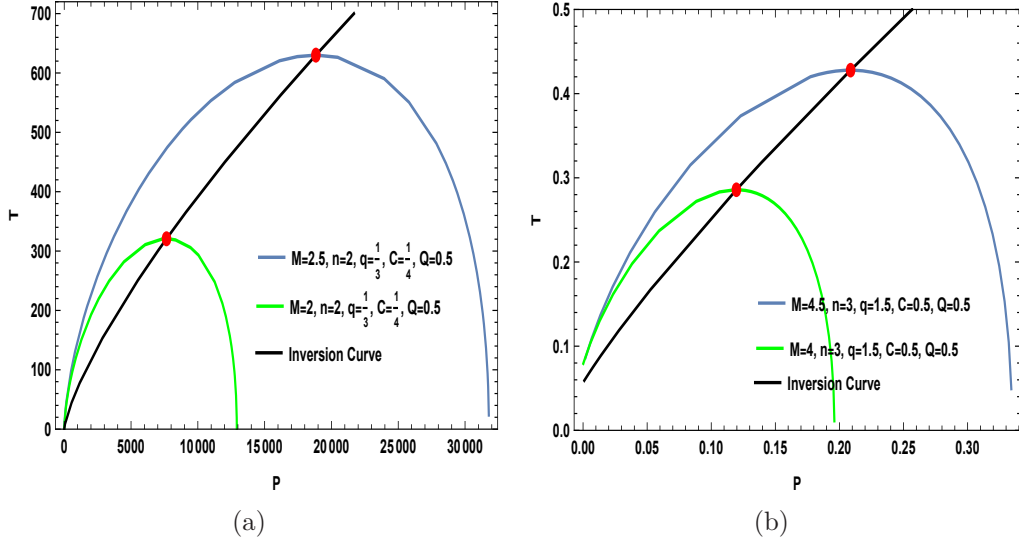


Figure 2: Isenthalpic curves and inversion curve of the AMPYM black hole with respect to mentioned free parameters that determine in each plot.

do not present the explicit expressions of the solutions here, as they are too long and complex. However, we can illustrate the relation between the inversion temperature T_i and the inversion pressure P_i by using the equations given above. Figure 3 shows the inversion curves for different free parameters. The inversion curve has only one branch. The inversion temperature rises steadily with the inversion pressure, but the slope of the inversion curves becomes smaller. We can also notice some fine structures in the cases of subfigures 3. For low pressure, the inversion temperature varies with the free parameters that are specified in each plot. It was interesting for us to study the effect of parameters and we observed that the slope of the inversion curve increases with the changes in the various values of each of the parameters.

Before the end of this section, if we want to talk purely about the effect of Maxwell charges as a specific result of our work, we should say that in [3], the authors found that for $q > 1$ and $n = 2$, the ratio T_i^{min}/T_c is fully established, but in the present work, by adding the Maxwell charge to the mentioned black hole, we found that for $C \gg 1$ the Yang–Mills parameter has no effect on the ratio, and in any case, the T_i^{min}/T_c is equal to $1/2$, which has the same behavior as a four-dimensional charged black hole. For $q > 1$, when C increases, the T_{min}/T_c approaches the value of $1/2$. However, for $q < 1$, the conditions are slightly different from the previous situation, because when $q = 1/2$, $n = 2$, and $Q_1 = 1$, the T_i^{min}/T_c is equal to $1/2$ for all values of "C", which is the same as a charged black hole in four dimensions. Also, according to Table 1 to 3, it can be inferred that when $1/2 < q < 1$, with the increase of Maxwell charge, i.e. C , the T_i^{min}/T_c only approaches the value of $1/2$ and exhibits a more similar behavior to a four-dimensional charged black hole. If for $0 < q < 1/2$, the T_i^{min}/T_c

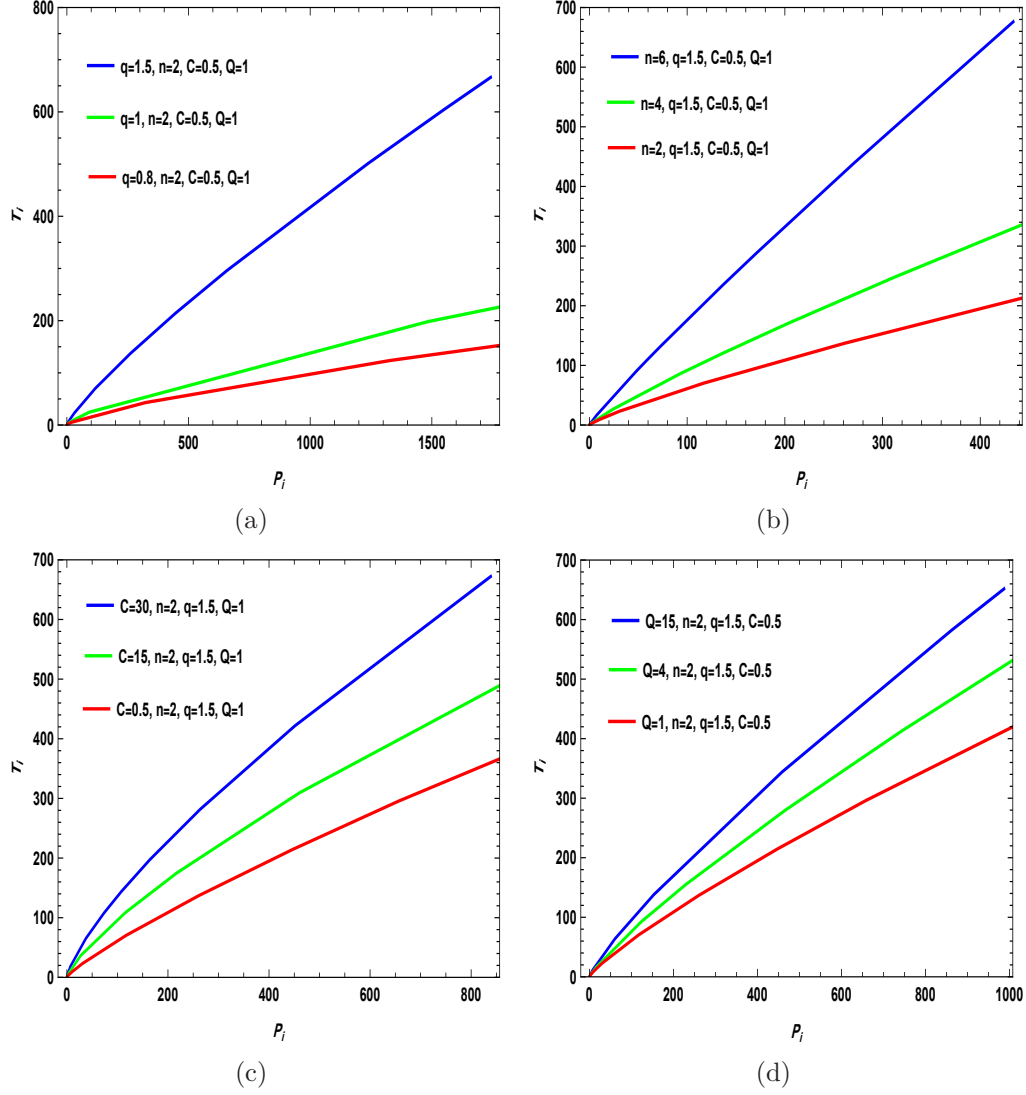


Figure 3: It shows the plot of The inversion curve for the AMPYM black hole with respect to free parameters that are determined in each plot

becomes further or smaller than the value of $1/2$, which is contrary to a charged black hole in four dimensions. In general, when $q > 1$, for the increase of Maxwell's charge C , the T_i^{min}/T_c is almost equal to $1/2$ and when $q = 1/2$, for all values of the Maxwell's charge, the T_i^{min}/T_c is equal to $1/2$. Also, when $1 < q < 1/2$, it is close to the value of $1/2$ and finally when $1/2 < q < 0$, the values of the T_i^{min}/T_c become smaller than of $1/2$.

5.2 Case II

With respect to [62, 78] and the Mass of black holes, We can express pressure P in terms of M and r_+ and replace it in the formula for the temperature, which will also become in terms of M and r_+ . We also rewrite the mass M and temperature T as a function of the pressure P and the radius r_+ of a black hole. So we will have,

$$P(M, r_+) = -\frac{3(a^2 + r_+(2b - 2\Xi^2 M + r_+))}{8\pi r_+(2b + r_+)(a^2 + r_+(2b + r_+))}. \quad (26)$$

Also, the temperature in terms of M and r_+ is as follows [62, 78],

$$\begin{aligned} \mathcal{X} &= a^4(b + r_+) + a^2 r_+(4b^2 + 6br_+ + r_+(2r_+ - \Xi^2 M)) + r_+^2(2b + r_+)(3r_+(b - \Xi^2 M) + 2b(b - \Xi^2 M) + r_+^2) \\ \mathcal{Y} &= 2\pi r_+(2b + r_+)(a^2 + 2br_+ + r_+)(a^2 + r_+(2b + r_+)) \\ T(M, r_+) &= -\frac{\mathcal{X}}{\mathcal{Y}}. \end{aligned} \quad (27)$$

Therefore, by using the equation (19) on can obtain,

$$\begin{aligned} \mathcal{A} &= a^8(2b^2 + 2br_+ + r_+^2) + a^6 r_+(16b^3 + 2b^2(9r_+ + 2) + br_+(2e^2 M + 8r_+ + 5) + r_+^2(r_+ + 2)) + a^4 r_+^2 \\ &\left[48b^4 + 4b^3(2\Xi^2 M + 16r_+ + 5) + 4b^2 r_+(8\Xi^2 M + 7r_+ + 8) + br_+^2(20\Xi^2 M + 2r_+ + 19) \right. \\ &\left. - r_+^2(\Xi^2(M - 4Mr_+) + (r_+ - 4)r_+) \right] + a^2 r_+^3(2b + r_+) \left[32b^4 + 4b^3(9r_+ + 4) + 2b^2 r_+(8\Xi^2 M + 5r_+ + 11) \right. \\ &\left. + br_+(4\Xi^2 M(r_+ + 1) + r_+(11 - 2r_+)) - (r_+ - 2)r_+^3 \right] \\ &+ (2b + 1)r_+^4(2b + r_+)^2 \left[4b^2(b - \Xi^2 M) + r_+^2(b - 3\Xi^2 M) + 4br_+(b - \Xi^2 M) \right] \\ \mathcal{B} &= \left[2\pi r_+^2(2b + r_+)^2(a^2 + r_+ + 2br_+)^2(a^2 + r_+(2b + r_+))^2 \right] \\ \mathcal{C} &= 3 \left[a^4(b + r_+) + a^2 r_+(4b^2 + 6br_+ + r_+(2r_+ - \Xi^2 M)) + r_+^2(2b + r_+)(3r_+(b - \Xi^2 M) + 2b(b - \Xi^2 M) + r_+^2) \right] \\ \mathcal{D} &= 4\pi r_+^2(2b + r_+)^2(a^2 + r_+(2b + r_+))^2 \\ \mu &= \frac{\mathcal{A}/\mathcal{B}}{\mathcal{C}/\mathcal{D}}. \end{aligned} \quad (28)$$

We express the mass M and temperature T in terms of the pressure P and the radius r_+ of a black hole, using different equations,

$$M(P, r_+) = \frac{(a^2 + r_+(2b + r_+))(8\pi pr_+(2b + r_+) + 3)}{6\Xi^2 r_+}, \quad (29)$$

$$T(P, r_+) = \frac{a^2 (8\pi p r_+^2 - 3) + r_+^2 (8\pi p (2b + r_+) (2b + 3r_+) + 3)}{12\pi r_+ (a^2 + 2br_+ + r_+)}. \quad (30)$$

The $V(P)$ for the AKS black hole is calculated as follows,

$$V(P) = \frac{4\pi(2b + r_+) (a^2 + r_+(2b + r_+))}{3\Xi^2}. \quad (31)$$

So, by using the equation (19), (21), (22) and (23) one can obtain,

$$\begin{aligned} T_i &= (2b + r_+) (a^2 + r_+(2b + r_+)) \\ &\times \left[a^4 (8\pi P_i r_+^2 + 3) + a^2 r_+ \left(32\pi b^2 P_i r_+ + 4b(32\pi P_i r_+^2 + 3) + 3(24\pi P_i r_+^3 + r_+ + 2) \right) \right. \\ &\left. + 16\pi(2b + 1) P_i r_+^4 (4b + 3r_+) \right] \\ &\left/ 12\pi r_+^2 (a^2 + 2br_+ + r_+)^2 (a^2 + (2b + r_+)(2b + 3r_+)) \right. \end{aligned} \quad (32)$$

Also, with respect to equation (30) we will have,

$$T_i = \frac{a^2 (8\pi r_+^2 P_i - 3) + r_+^2 (8\pi P (2b + r_+) (2b + 3r_+) + 3)}{12\pi r_+ (a^2 + 2br_+ + r_+)}. \quad (33)$$

We have drawn the isenthalpic curves and the inversion curve of the AdS Kerr Sen black hole for various free parameter values in each plot of Figure 4. In every subfigure, three isenthalpic curves with different M are visible, along with the corresponding inversion curve that occurs at the highest point of the isenthalpic curves. We denote each isenthalpic curve's inversion temperature and pressure as T_i and P_i , respectively. The isenthalpic curves are divided into two regions by the inversion curve: for $P < P_i$, the isenthalpic curve has a positive slope, indicating that the black hole undergoes cooling during the expansion process. With the changes in the parameters of the black hole, we found that the slope of the figures will change, and these changes are visible in each subfigure. Because an analytical solution is difficult to obtain, we used a numerical method to draw graphs. If we assume the parameter b to be zero, our equations and graphs will simplify to the Kerr-AdS black holes, whose results are thoroughly discussed in [1]. Due to the complexity of the calculations, we do not show the explicit expressions here. However, we can demonstrate the relation between the inversion temperature T_i and the inversion pressure P_i by using the equations given above. Figure (5a-5d) displays the inversion curves for different free parameters of the AKS black holes. The inversion curve has only one branch. The inversion temperature increases gradually with the inversion pressure, but the slope of the inversion curves becomes smaller. We can also observe some fine structures in the cases of subfigures 5. Inversion curves change with the free parameters that are specified in each plot. It was very difficult to find the analytical solution for drawing the graphs, so we used numerical solutions to draw them. Moreover, we note that due to the huge difference in the values of the horizontal and vertical graphs corresponding to the change of the free parameters, we have drawn the figures separately. In Figure 6, we plot the Hawking temperature as a function of the horizon, which is the

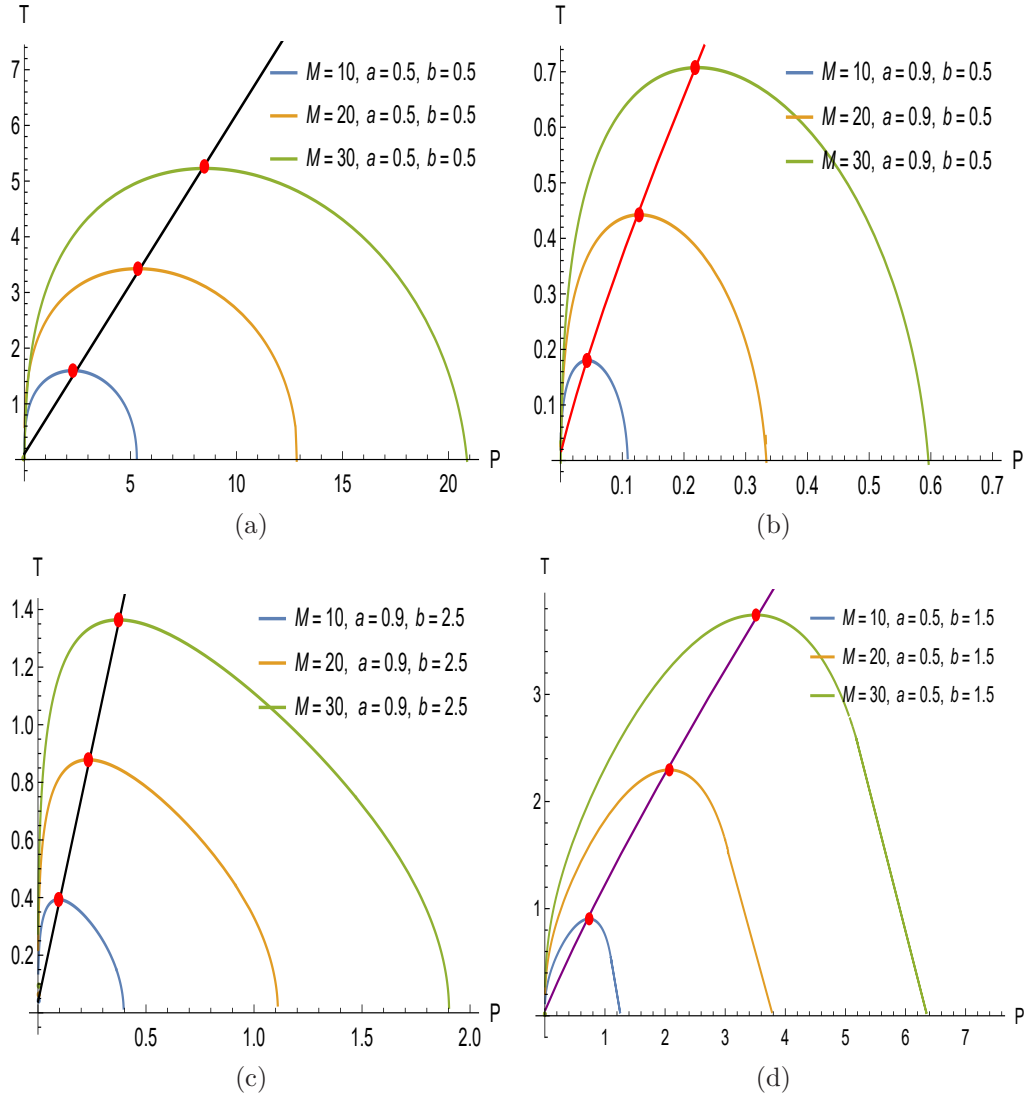


Figure 4: Isenthalpic curves and inversion curve of the AdS-Ker-Sen black hole with respect to mentioned free parameters that determine in each plot.

boundary of the black hole. The horizon can be affected by the presence of other fields or dimensions, which are represented by the free parameters in our model. We consider the free parameters constant for each plot, but we vary them across different plots to see how they influence the Hawking temperature. In each subfigure, we can observe some zero points, where the Hawking temperature becomes zero for different free parameters. This means that the black hole became extremal at these points. These zero points correspond to the divergence points of the JTC, which is a quantity that describes the temperature change when a gas expands or compresses at constant enthalpy. In the study of Kerr black hole [1], it was shown that the rotation parameter "a" does not

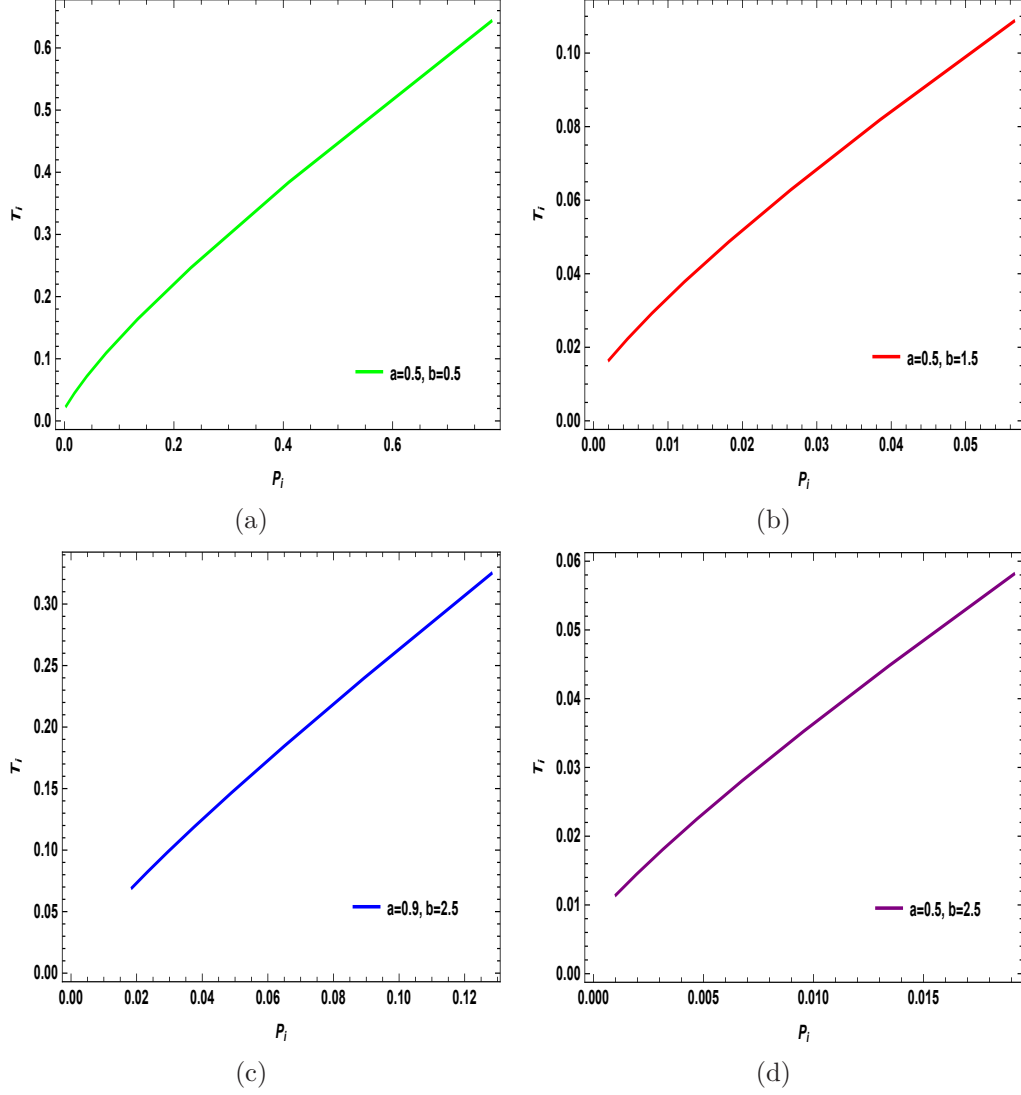


Figure 5: It shows the plot of The inversion curve for the AdS-Ker-Sen black hole with respect to free parameters that are determined in each plot with $M=20$

have much effect on the Joule-Thomson representation. For example, it is practically eliminated in the ratio of the T_i^{min}/T_C , and the value of this ratio is always a constant value of $1/2$. In this paper, we found that the parameters related to AKS black hole, i.e. a and b , can play a vital role in the representation of the value of the T_i^{min}/T_C . The value of this ratio increases with the reduction of these parameters. For this purpose, due to the structural complexities of this black hole, we could not use the analytical method to obtain the critical points of the black hole, so we resorted to the approximate method and the numerical calculations. In the [77], the value of critical temperature and critical pressure has been calculated. We calculated some values for this black hole

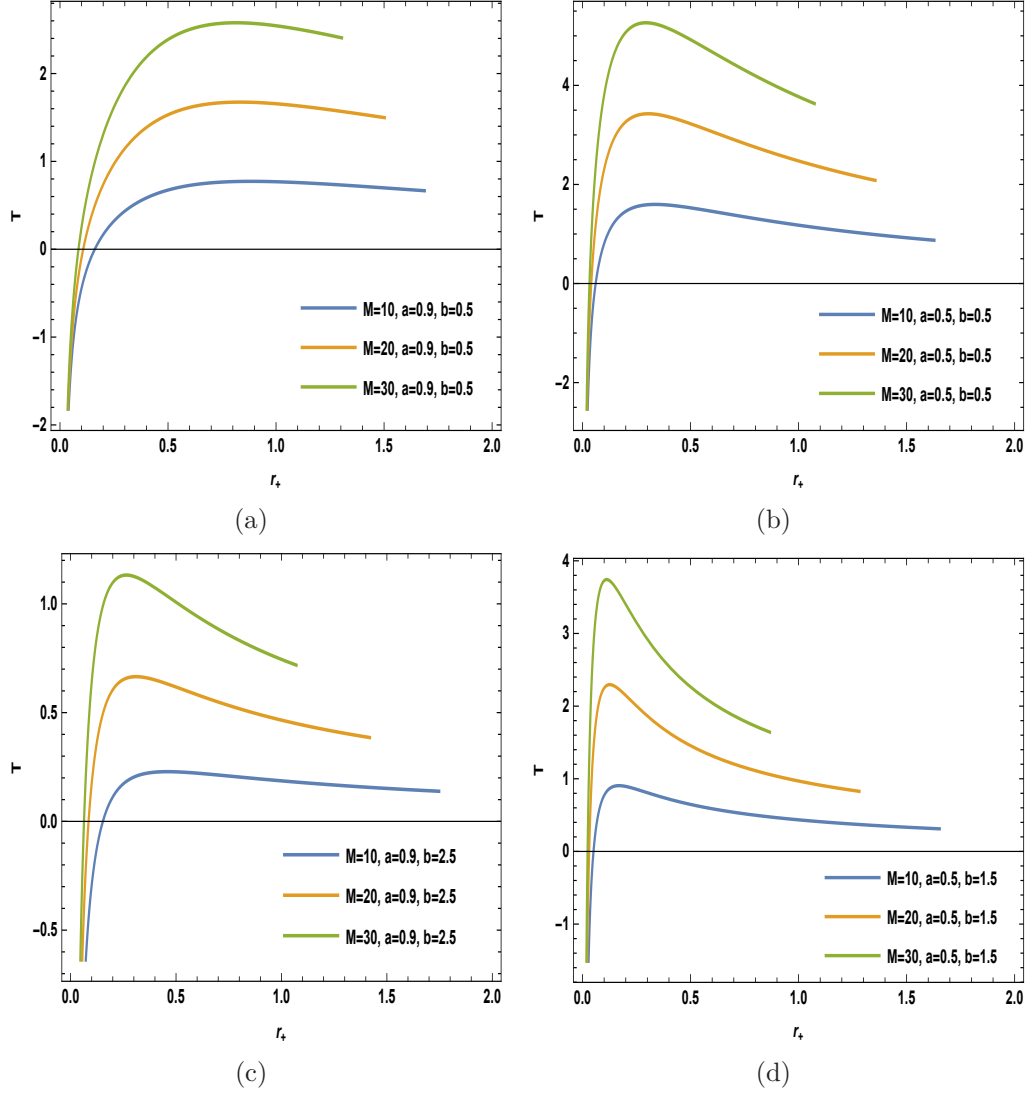


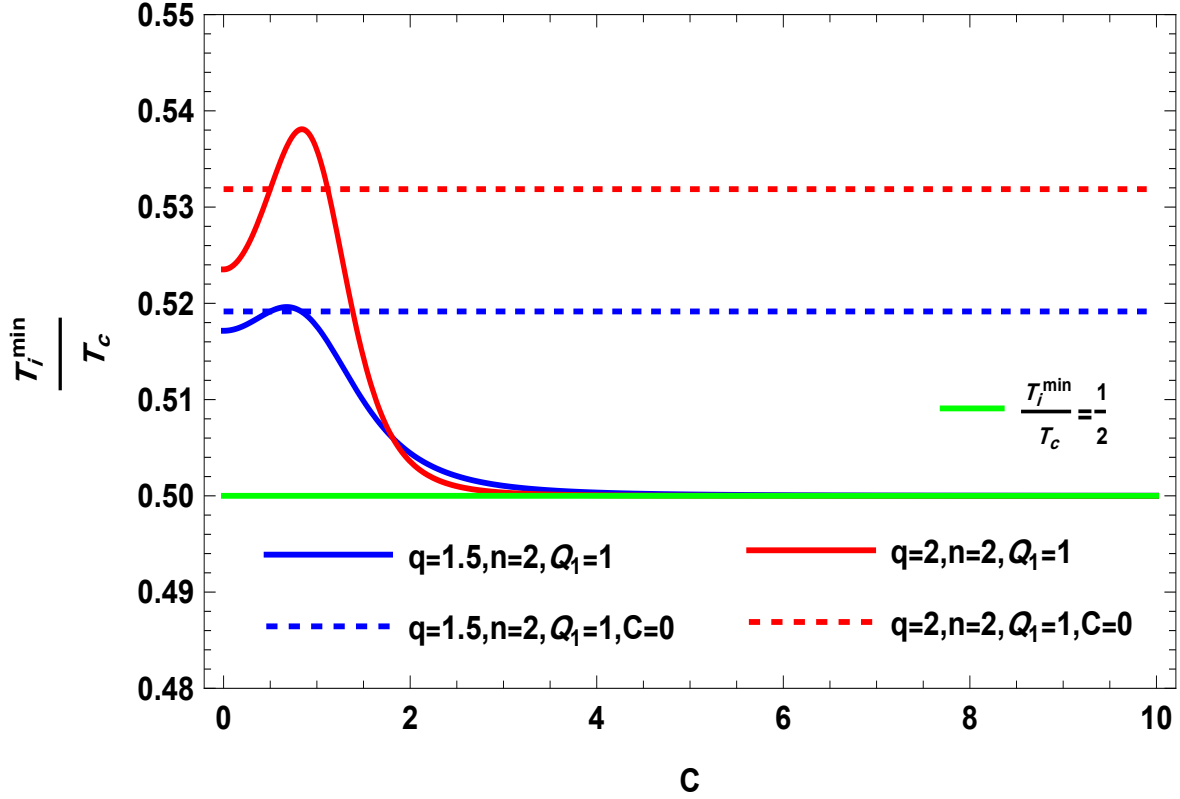
Figure 6: It shows the plot of $(T - r_+)$ for the AdS-Ker-Sen black hole with respect to free parameters that are determined in each plot

according to Table 4. As evident, regarding various values of free parameters, the T_i^{min}/T_C is obtained, which shows the obvious effect of parameters a and b .

6 Conclusion

In this article, we investigated the behavior of two structurally different black holes under the JTE thermodynamic process. The JTE is a process that cools or heats a system by changing its pressure and volume at constant enthalpy, and its main goal is to study the behavior of the μ coefficient, which describes the change in temperature during the expansion or compression of a system. But before presenting the results, we must first explain the motivations that led us to choose these particular black holes. Recently, Einstein-Power-Young-Mills black hole with AdS structure under JTE process was investigated in a research paper [2, 3]. This raised the question in our mind that if a fields in the Maxwellian form are added to the elements in the action of the above article, can this change and addition of a special form of the field cause a different thermodynamic behavior in their JT representation? Similarly, in the past, the behavior of various forms of rotating black holes was also investigated in this thermodynamic process. But what effect can the addition of Sen-type dilaton fields and antisymmetric tensor fields have on its thermodynamic properties and JT representation? This was a question that could be a good motivation for our investigation. For this purpose, we plotted the isenthalpic curves and the inversion curves for each of the two black holes, for different values of the free parameters, which can be referred to the following results for each. For the AMPYM black hole, the Hawking temperature has zero points that depend on the free parameters and the horizon radius, and the JTC diverges at these points. The isenthalpic curves are divided into two regions by the inversion curve: for $P < P_i$, the isenthalpic curve has a positive slope, indicating that the black hole is cooling during the expansion process, and for $P > P_i$, the isenthalpic curve has a negative slope, which means that the black hole experiences heating during the expansion process. The inversion curves for different free parameters show that the inversion curve has only one branch and the inversion temperature increases steadily with the inversion pressure, but the slope of the inversion curves becomes smaller. Also, the graphs showed that for low pressure, the inversion temperature varies with the free parameters specified in each graph. Studying the effect of parameters was interesting for us because we observed that the slope of the inversion curve increases with changes in different values of each parameter. *But if we want to talk about the effect of Maxwell's charges as a special result of our work, we must state that, we have found that the ratio of minimum to critical temperature for a 4-dimensional black hole with Yang-Mills hair depends on the values of q , M , and C . For $q > 1$, the ratio is almost equal to $1/2$ regardless of the Yang-Mills parameter when " $C \gg 1$ ". For $q = 1/2$, the ratio is exactly equal to $1/2$ for all values of C . For $1/2 < q < 1$, the ratio approaches $1/2$ as C increases. For $0 < q < 1/2$, the ratio deviates from $1/2$ as C increases. These results show that the Maxwell charge can affect the thermodynamic behavior of the black hole and make it more or less similar to a 4-dimensional charged black hole. Also, for the AKS black hole, we found that its parameters, i.e. a and b , can play a vital role in the representation of the value of the ratio of T_i^{min}/T_C , so that by reducing these parameters, the value of the ratio increases.* The results are shown in Figure 7 and are summarized in Tables 1 to 5. For the AdS Kerr Sen black, It was very difficult to find the analytical solution for drawing the graphs, so we used numerical solutions to draw them. For $P < P_i$, the isenthalpic curve has a positive slope, indicating that the black hole is cooling during the expansion process, but with the increases of the black hole parameters, we found that the slope of the figures will change. Also, if we assume the parameter b (dyonic charge) to be zero, our equations and graphs will simplify to the Kerr-AdS black holes, whose results are thoroughly discussed in [1]. In general, it can be said about this black hole the isenthalpic curves of the

AKS black hole show cooling or heating behavior depending on the inversion curve, which is affected by the mass and the parameter b, a of the black hole. The inversion curve has a single branch with a positive slope that decreases with the free parameters, and the inversion temperature and pressure are related by some equations that are numerically solved. The Hawking temperature of the AKS black hole has zero points that depend on the free parameters and the horizon radius and lead the JTC to reflect divergence behavior.



(a)

Figure 7: It shows the plot of $(\frac{T_i^{min}}{T_c})$ in terms of C with respect to free parameters mentioned in the plot.

$q = 0.3, n = 2, Q_1 = 1$	T_i^{min}	T_c	T_i^{min}/T_c
$C = 0.1$	0.171532	0.355378	0.482674
$C = 0.2$	0.068796	0.148927	0.461947
$C = 0.3$	0.035473	0.082056	0.432299
$C = 1$	Not Exist	Not Exist	Not Exist
$C = 5$	Not Exist	Not Exist	Not Exist
$C = 10$	Not Exist	Not Exist	Not Exist

Table 1: Summary of the results for the AMPYM black hole for $q = 0.3$

$q = 0.5, n = 2, Q_1 = 1$	T_i^{min}	T_c	T_i^{min}/T_c
$C = 0.1$	0.034331	0.068662	0.5
$C = 0.2$	0.017165	0.034330	0.5
$C = 0.3$	0.011443	0.022886	0.5
$C = 1$	0.003433	0.006866	0.5
$C = 5$	0.000686	0.001372	0.5
$C = 10$	0.000343	0.000686	0.5

Table 2: Summary of the results for the AMPYM black hole for $q = 0.5$

$q = 0.9, n = 2, Q_1 = 1$	T_i^{min}	T_c	T_i^{min}/T_c
$C = 0.1$	0.019146	0.03874	0.493657
$C = 0.2$	0.018873	0.038208	0.493962
$C = 0.3$	0.018446	0.037309	0.494405
$C = 1$	0.013846	0.027832	0.497502
$C = 5$	0.004141	0.008286	0.499762
$C = 10$	0.002133	0.004267	0.499921

Table 3: Summary of the results for the AMPYM black hole for $q = 0.9$

(a, b)	T_i^{min}	T_c	T_i^{min}/T_c
(0.0099, 0.00499)	0.0787687	0.335030	0.235109
(0.00972, 0.00486)	0.0782007	0.2302899	0.33957
(0.00951, 0.00475)	0.078821	0.156982	0.5
(0.00937, 0.00468)	0.0788340	0.116006	0.67379
(0.00892, 0.00442)	0.776375	0.0454247	1.709

Table 4: Summary of the results for the AKS black hole

AMPYM BH	$q > 1, C \gg 1$	$T_{min}/T_c = \frac{1}{2}$	This paper
AMPYM BH	$q = 0.5$, all values of "C"	$T_{min}/T_c \simeq \frac{1}{2}$	This paper
AMPYM BH	$0.5 < q \leq 1$, $C \gg 1$	$T_{min}/T_c \simeq \frac{1}{2}$	This paper
AKS BH	$(a = 0.00951,$ $b = 0.00475)$	$T_{min}/T_c \simeq \frac{1}{2}$	This paper
Van der Waals fluid	Exist	$T_{min}/T_c = \frac{3}{4}$	[24]
RN-AdS BH	Exist	$T_{min}/T_c = \frac{1}{2}$	[25]
d-dimensional AdS BH	Exist	$T_{min}/T_c < \frac{1}{2}$	[79]
Gauss-Bonnet BH	Exist	$T_{min}/T_c = 0.4765$	[80]
torus-like BH	Not Exist	$T_{min}/T_c =$ Not Exist	[81]
BTZ BH	Not Exist	$T_{min}/T_c =$ Not Exist	[82]

Table 5: Summary of the results for the AMPYM and AKS black holes compare with other results

References

- [1] Ökcü, Özgür, and Ekrem Aydiner. "Joule–Thomson expansion of Kerr–AdS black holes." *The European Physical Journal C* 78 (2018): 1-6.
- [2] Du, Yun-Zhi, et al. "Nonlinearity effect on Joule–Thomson expansion of Einstein–Power–Yang–Mills AdS black hole." *The European Physical Journal C* 83.5 (2023): 426.
- [3] Biswas, Anindya. "Joule-Thomson expansion of AdS black holes in Einstein Power-Yang-mills gravity." *Physica Scripta* 96.12 (2021): 125310.
- [4] Bekenstein, Jacob D. "Black holes and entropy." *Physical Review D* 7.8 (1973): 2333.
- [5] Bardeen, James M., Brandon Carter, and Stephen W. Hawking. "The four laws of black hole mechanics." *Communications in mathematical physics* 31 (1973): 161-170.
- [6] Hawking, Stephen W. "Particle creation by black holes." *Communications in mathematical physics* 43.3 (1975): 199-220.
- [7] Maldacena, Juan. "The large-N limit of superconformal field theories and supergravity." *International journal of theoretical physics* 38.4 (1999): 1113-1133.
- [8] Gubser, Steven S., Igor R. Klebanov, and Alexander M. Polyakov. "Gauge theory correlators from non-critical string theory." *Physics Letters B* 428.1-2 (1998): 105-114.
- [9] Witten, Edward. "Anti de Sitter space and holography." arXiv preprint hep-th/9802150 (1998).
- [10] Hawking, Stephen W., and Don N. Page. "Thermodynamics of black holes in anti-de Sitter space." *Communications in Mathematical Physics* 87 (1983): 577-588.
- [11] Witten, Edward. "Anti-de Sitter space, thermal phase transition and confinement in gauge theories." *International Journal of Modern Physics A* 16.16 (2001): 2747-2769.
- [12] Chamblin, Andrew, et al. "Charged AdS black holes and catastrophic holography." *Physical Review D* 60.6 (1999): 064018.
- [13] Chamblin, Andrew, et al. "Holography, thermodynamics, and fluctuations of charged AdS black holes." *Physical Review D* 60.10 (1999): 104026.
- [14] Banerjee, Rabin, Sujoy Kumar Modak, and Dibakar Roychowdhury. "A unified picture of phase transition: from liquid-vapour systems to AdS black holes." *Journal of High Energy Physics* 2012.10 (2012): 1-11.
- [15] Kastor, David, Sourya Ray, and Jennie Traschen. "Enthalpy and the mechanics of AdS black holes." *Classical and Quantum Gravity* 26.19 (2009): 195011.

- [16] Kubizank, David, and Robert B. Mann. "P-V criticality of charged AdS black holes." JHEP 2012. 7 (2012): 1-25.
- [17] Spallucci, Euro, and Anais Smailagic. "Maxwell's equal-area law for charged AdS black holes." PLB 723.4-5 (2013): 436-441.
- [18] Gunasekaran, Sharmila, David Kubizňák, and Robert B. Mann. "Extended phase space thermodynamics for charged and rotating black holes and Born-Infeld vacuum polarization." Journal of High Energy Physics 2012.11 (2012): 1-43.
- [19] Hendi, S., and M. Vahidinia. "P-V criticality of higher dimensional black holes with nonlinear source." arXiv preprint arXiv:1212.6128 (2012).
- [20] Chen, Song-Bai, Xiao-Fang Liu, and Chang-Qing Liu. "P—V criticality of an ads black hole in $f(r)$ gravity." Chinese Physics Letters 30.6 (2013): 060401.
- [21] Zhao, Ren, et al. "On the critical phenomena and thermodynamics of charged topological dilaton AdS black holes." The European Physical Journal C 73 (2013): 1-10.
- [22] Altamirano, Natacha, David Kubizňák, and Robert B. Mann. "Reentrant phase transitions in rotating anti-de Sitter black holes." Physical Review D 88.10 (2013): 101502.
- [23] Cai, Rong-Gen, et al. "PV criticality in the extended phase space of Gauss-Bonnet black holes in AdS space." Journal of High Energy Physics 2013.9 (2013): 1-22.
- [24] Ökcü, Özgür, and Ekrem Aydiner. "Joule–Thomson expansion of the charged AdS black holes." The European Physical Journal C 77 (2017): 1-7.
- [25] Ghaffarnejad, H., E. Yaraie, and M. Farsam. "Quintessence Reissner Nordström anti de Sitter black holes and Joule Thomson effect." International Journal of Theoretical Physics 57 (2018): 1671-1682.
- [26] D'Almeida, Roopa, and K. P. Yogendran. "Thermodynamic properties of holographic superfluids." arXiv preprint arXiv:1802.05116 (2018).
- [27] Chabab, Mohamed, et al. "Joule-Thomson Expansion of RN-AdS Black Holes in $f(R)$ gravity." arXiv preprint arXiv:1804.10042 (2018).
- [28] Ahmed Rizwan, C. L., et al. "Joule–Thomson expansion in AdS black hole with a global monopole." International Journal of Modern Physics A 33.35 (2018): 1850210.
- [29] Mo, Jie-Xiong, and Gu-Qiang Li. "Effects of Lovelock gravity on the Joule–Thomson expansion." Classical and Quantum Gravity 37.4 (2020): 045009.
- [30] Zhang, Meng-Yao, et al. "Joule-Thomson expansion of charged dilatonic black holes." Chinese Physics C 47.4 (2023): 045101.

- [31] Gogoi, Dhruva Jyoti, et al. "Joule-Thomson Expansion and Optical Behaviour of Reissner-Nordström-Anti-de Sitter Black Holes in Rastall Gravity Surrounded by a Quintessence Field." *Fortschritte der Physik* 71.4-5 (2023): 2300010.
- [32] Meng, Yuan, Jin Pu, and Qing-Quan Jiang. "PV criticality and Joule-Thomson expansion of charged AdS black holes in the Rastall gravity." *Chinese Physics C* 44.6 (2020): 065105.
- [33] Lekbich, H., et al. "4D AdS Einstein–Gauss–Bonnet black hole endowed with Lorentzian noncommutativity: P-V criticality, Joule–Thomson expansion, and shadow." *Annals of Physics* 458 (2023): 169451.
- [34] Kruglov, S. I. "Magnetically Charged AdS Black Holes and Joule–Thomson Expansion." *Gravitation and Cosmology* 29.1 (2023): 57-61.
- [35] Kruglov, S. I. "Magnetic black holes in AdS space with nonlinear electrodynamics, extended phase space thermodynamics and Joule-Thomson expansion." *International Journal of Geometric Methods in Modern Physics* 20.01 (2023): 2350008.
- [36] Graça, JP Morais, et al. "Joule-Thomson expansion for quantum corrected AdS-Reissner-Nördstrom black holes in a Kiselev spacetime." *Physical Review D* 107.2 (2023): 024045.
- [37] Kruglov, Sergey Il'ich. "Einstein-AdS Gravity Coupled to Nonlinear Electrodynamics, Magnetic Black Holes, Thermodynamics in an Extended Phase Space and Joule–Thomson Expansion." *Universe* 9.10 (2023): 456.
- [38] Arora, Dhruv, et al. "Joule-Thomson expansion and tidal force effects of AdS black holes surrounded by Chaplygin dark fluid." arXiv preprint arXiv:2312.16224 (2023).
- [39] El Mounni, H. "Revisiting the phase transition of AdS-Maxwell–power-Yang–Mills black holes via AdS/CFT tools." *Physics Letters B* 776 (2018): 124-132.
- [40] Zhang, Ming, et al. "P–V criticality of AdS black hole in the Einstein–Maxwell–power-Yang–Mills gravity." *General Relativity and Gravitation* 47.2 (2015): 14.
- [41] Pippard, Alfred Brian. *Elements of classical thermodynamics: for advanced students of physics*. Cambridge University Press, 1964.
- [42] Yasskin, Philip B. "Solutions for gravity coupled to massless gauge fields." *Physical Review D* 12.8 (1975): 2212.
- [43] Kasuya, Masahiro. "Exact solution of a rotating dyon black hole." *Physical Review D* 25.4 (1982): 995.
- [44] Mazharimousavi, S. Habib, and Mustafa Halilsoy. "5D black hole solution in Einstein-Yang-Mills-Gauss-Bonnet theory." *Physical Review D* 76.8 (2007): 087501.

- [45] Mazharimousavi, S. Habib, and Mustafa Halilsoy. "Einstein–Yang–Mills black hole solution in higher dimensions by the Wu–Yang ansatz." *Physics Letters B* 659.3 (2008): 471-475.
- [46] Mazharimousavi, S. Habib, Mustafa Halilsoy, and Zahra Amirabi. "New non-Abelian black hole solutions in Born-Infeld gravity." *Physical Review D* 78.6 (2008): 064050.
- [47] Ghosh, Sushant G. "5D radiating black holes in Einstein–Yang–Mills–Gauss–Bonnet gravity." *Physics Letters B* 704.1-2 (2011): 5-9.
- [48] Bartnik, Robert, and John McKinnon. "Particlelike solutions of the Einstein-Yang-Mills equations." *Physical Review Letters* 61.2 (1988): 141.
- [49] Bizon, Piotr. "Colored black holes." *Physical review letters* 64.24 (1990): 2844.
- [50] Galt'sov, D. V., and A. A. Ershov. "Non-Abelian baldness of colored black holes." *Physics Letters A* 138.4-5 (1989): 160-164.
- [51] Volkov, Mikhail S., and Dimitri V. Gal'Tsov. "Black holes in Einstein-Yang-Mills theory." *Soviet Journal of Nuclear Physics* 51.4 (1990): 747-753.
- [52] Straumann, Norbert, and Zhi-Hong Zhou. "Instability of the Bartnik-McKinnon solution of the Einstein-Yang-Mills equations." *Physics Letters B* 237.3-4 (1990): 353-356.
- [53] Zhou, Zhi-hong, and Norbert Straumann. "Nonlinear perturbations of Einstein-Yang-Mills solitons and non-Abelian black holes." *Nuclear Physics B* 360.1 (1991): 180-196.
- [54] Volkov, M. S., et al. "Cosmological analogues of the Bartnik-McKinnon solutions." *Physical Review D* 54.12 (1996): 7243.
- [55] Winstanley, E. "Existence of stable hairy black holes in $su(2)$ Einstein-Yang-Mills theory with a negative cosmological constant." *Classical and Quantum Gravity* 16.6 (1999): 1963.
- [56] Bjoraker, Jefferson, and Yutaka Hosotani. "Stable Monopole and Dyon Solutions in the Einstein-Yang-Mills Theory in Asymptotically anti-de Sitter Space." *Physical Review Letters* 84.9 (2000): 1853.
- [57] Bjoraker, Jeff, and Yutaka Hosotani. "Monopoles, dyons, and black holes in the four-dimensional Einstein-Yang-Mills theory." *Physical Review D* 62.4 (2000): 043513.
- [58] Stetsko, M. M. "Static spherically symmetric black hole in Einstein-power-Yang-Mills-dilaton theory and some aspects of its thermodynamics." *arXiv preprint arXiv:2012.14902* (2020).
- [59] Gogoi, Dhruva Jyoti, et al. "Quasinormal Modes and Optical Properties of 4-D black holes in Einstein Power-Yang-Mills Gravity." *arXiv preprint arXiv:2306.14273* (2023).

- [60] El Mounni, H. "Revisiting the phase transition of AdS-Maxwell-power-Yang-Mills black holes via AdS/CFT tools." *Physics Letters B* 776 (2018): 124-132.
- [61] Sen, Ashoke. "Rotating charged black hole solution in heterotic string theory." *Physical Review Letters* 69.7 (1992): 1006.
- [62] Ali, Md Sabir, Sushant G. Ghosh, and Anzhong Wang. "Thermodynamics of Kerr-Sen-AdS black holes in the restricted phase space." *Physical Review D* 108.4 (2023): 044045.
- [63] Zhang, Meng-Yao, et al. "Thermodynamic topology of Kerr-Sen black holes via Rényi statistics." arXiv preprint arXiv:2312.12814 (2023).
- [64] Wu, Di, et al. "Aspects of the dyonic Kerr-Sen-AdS₄ black hole and its ultraspinning version." *Physical Review D* 103.4 (2021): 044014.
- [65] Narang, Ashish, Subhendra Mohanty, and Abhass Kumar. "Test of Kerr-Sen metric with black hole observations." arXiv preprint arXiv:2002.12786 (2020).
- [66] Prihadi, Hadyan Luthfan, et al. "Chaos and fast scrambling delays of dyonic Kerr-Sen-AdS₄ black hole and its ultra-spinning version." arXiv preprint arXiv:2304.08751 (2023).
- [67] Sakti, Muhammad FAR, and Piyabut Burikham. "Dual CFT on a dyonic Kerr-Sen black hole and its gauged and ultraspinning counterparts." *Physical Review D* 106.10 (2022): 106006.
- [68] Sakti, Muhammad Fitrah Alfian Rangga. "Hidden conformal symmetry for dyonic Kerr-Sen black hole and its gauged family." *The European Physical Journal C* 83.3 (2023): 255.
- [69] Siahaan, Haryanto M. "Instability of charged massive scalar fields in bound states around Kerr-Sen black holes." *International Journal of Modern Physics D* 24.14 (2015): 1550102.
- [70] Hioki, Kenta, and Umpei Miyamoto. "Hidden symmetries, null geodesics, and photon capture in the Sen black hole." *Physical Review D* 78.4 (2008): 044007.
- [71] Jiang, Jie, Xiaoyi Liu, and Ming Zhang. "Examining the weak cosmic censorship conjecture by gedanken experiments for Kerr-Sen black holes." *Physical Review D* 100.8 (2019): 084059.
- [72] Sakti, Muhammad Fitrah Alfian Rangga. Dual CFT on Nariai limit for Kerr-Sen-dS black holes. No. arXiv: 2307.04929.
- [73] Wu, Di, et al. "Are ultraspinning Kerr-Sen-AdS₄ black holes always superentropic?." *Physical Review D* 102.4 (2020): 044007.
- [74] Gibbons, Gary W., and Kei-ichi Maeda. "Black holes and membranes in higher-dimensional theories with dilaton fields." *Nuclear Physics B* 298.4 (1988): 741-775.

- [75] Garfinkle, David, Gary T. Horowitz, and Andrew Strominger. "Charged black holes in string theory." *Physical Review D* 43.10 (1991): 3140.
- [76] Zhang, Ming, and Jie Jiang. "Strong cosmic censorship in near-extremal Kerr-Sen-de Sitter spacetime." *The European Physical Journal C* 81 (2021): 1-8.
- [77] Sharif, M., and Qanita A-Tul-Mughani. "P-V criticality and phase transition of the Kerr-Sen-AdS black hole." *The European Physical Journal Plus* 136.3 (2021): 284.
- [78] Sakti, Muhammad FAR, and Piyabut Burikham. "Dual CFT on a dyonic Kerr-Sen black hole and its gauged and ultraspinning counterparts." *Physical Review D* 106.10 (2022): 106006.
- [79] Mo, Jie-Xiong, et al. "Joule-Thomson expansion of d-dimensional charged AdS black holes." *Physical Review D* 98.12 (2018): 124032.
- [80] Lan, Shan-Quan. "Joule-Thomson expansion of charged Gauss-Bonnet black holes in AdS space." *Physical Review D* 98.8 (2018): 084014.
- [81] Liang, Jing, Wei Lin, and Benrong Mu. "Joule-Thomson expansion of the torus-like black hole." *The European Physical Journal Plus* 136.11 (2021): 1169.
- [82] Liang, Jing, Benrong Mu, and Peng Wang. "Joule-Thomson expansion of lower-dimensional black holes." *Physical Review D* 104.12 (2021): 124003.